ELSEVIER

Catalysis Today 43 (1998) 79–88

CATALYSIS TODAY

The preparation of high surface area CeO_2–ZrO_2 mixed oxides by a surfactant-assisted approach

Daniela Terribile[a], Alessandro Trovarelli[a,*], Jordi Llorca[b], Carla de Leitenburg[a], Giuliano Dolcetti[a]

[a] *Dipartimento di Scienze e Tecnologie Chimiche, Università di Udine, via Cotonificio 108, 33100 Udine, Italy*
[b] *Departament de Química Inorgànica, Universitat de Barcelona, Diagonal 647, 08028 Barcelona, Spain*

Abstract

The study investigates the preparation of high surface area, three-way catalysts (TWC)-like, ceria–zirconia mixed oxide. It is shown that under basic conditions cationic surfactants effectively incorporate into hydrous oxides of cerium and zirconium. The presence of cerium inhibits the action of alkyl-trimethyl-ammonium salts as true templating agents and there is no formation of a regular pore structure. The elimination of surfactants upon calcination gives rise to the formation of high surface area, fluorite-structured CeO_2–ZrO_2 solid solution characterized by a fairly good compositional homogeneity. Surface areas in excess of 230 m^2/g were obtained after calcination at 723 K, which drop to ca. 40 m^2/g following treatment at 1173 K.

Keywords: Ceria–zirconia; CeO_2; ZrO_2; TWC; Mesoporous oxide; Auto-exhaust catalysts

1. Introduction

Materials containing ceria are attracting much attention because of their use either as catalysts and/or oxygen storage/release components in the formulation of catalysts for the control of emissions from automobiles [1]. A strong effort has been directed to increase the overall efficiency of CeO_2 in these applications and recently a new generation of mixed oxides based on CeO_2 and ZrO_2 has been developed [2,3]. Their effectiveness derives from the improvement of several features with respect to catalysts based on pure ceria: ceria–zirconia shows enhanced redox and oxygen storage properties [4,5]; improved thermal resistance [6]; and better catalytic activity at lower temperatures [7,8].

One of the keys to this success is the selection of appropriate preparation methods and composition (i.e. Ce/Zr ratio), which in turn determine homogeneity at a molecular level and textural/morphological properties. Several methods have recently been described for the preparation of CeO_2–ZrO_2 solid solutions for catalytic applications. These range from the high-temperature firing [2] or high-energy milling [9] of a mixture of the oxides, to conventional co-precipitation [10,11] and sol–gel techniques [4]. Materials across almost the entire composition range with varying degrees of homogeneity and textural properties have been prepared. Generally, Ce-rich compositions are preferred for the purposes of catalysis and the best results are obtained using $Ce_xZr_{1-x}O_2$ with x ranging

*Corresponding author. Fax: +39 432 558803; e-mail: trovarelli@dstc.uniud.it

0920-5861/98/$32.00
PII S0920-5861(98)00136-9

from 0.6 to 0.8. Of course, textural properties also play an important role in the development of these materials, especially when they are used for the deposition of noble metals [12]. The surface areas of ceria–zirconia obtained by conventional co-precipitation or sol/gel methods are typically in the range 60–90 m^2/g after calcination under air at 700–800 K [4,10]. Surface areas in excess of 100 m^2/g have been reported for materials obtained from CeO_2–ZrO_2 aerogels [13].

The use of templating techniques for the synthesis of mesoporous solids has recently opened up new opportunities in the design of novel high-surface area materials for catalytic applications. Much interest is being focused on the preparation of transition-metal oxides using several templating pathways [14–16]. Several meso-structured surfactant-oxide composites have been synthesized by this approach. A few of these composites showed a regular pore structure even after calcination [17,18] while the majority suffered from collapse of the regular pore structure after calcination [19]. Zirconia is currently under extensive investigation in this area and several different approaches have been developed, using cationic [20,21], anionic [22] or amphoteric routes [23], to expand the range of surface areas available.

This study is part of a project aimed at developing doped-ceria catalysts with improved textural, structural and chemical properties for environmental applications. In that context, we prepared high surface area ceria–zirconia using a surfactant-assisted approach. The preparation procedure was geared toward the application of ceria–zirconia as an oxygen storage/redox component and particular attention was given to homogeneity and stability issues, especially after thermal treatments.

2. Experimental

2.1. Materials

Two ceria–zirconia solid solutions of composition $Ce_{0.68}Zr_{0.32}O_2$ (CZ68) and $Ce_{0.80}Zr_{0.20}O_2$ (CZ80) were prepared by reaction of a cationic surfactant with the hydrous mixed oxide produced by co-precipitation under basic conditions. In a standard experiment the materials were prepared by adding an aqueous solution of the appropriate cationic surfactant (we used cetyltrimethylammonium bromide, C_{16}, 0.1 M, Aldrich) to an aqueous solution containing the stoichiometric quantities of $CeCl_3 \cdot 7H_2O$ (Aldrich) and $ZrOCl_2 \cdot 8H_2O$ (Aldrich) ([Ce]+[Zr]=0.1 M). The molar ratio ([Ce]+[Zr])/[C_{16}] was kept at 0.8. The mixture was stirred for 15 min and then aqueous ammonia (25%) was slowly added with vigorous stirring until the pH was 11.5. The addition of ammonia induced the precipitation of a gelatinous yellow–brown solid. The mixture was stirred for 60 min in a glass reactor, then sealed and placed in a thermostatic bath maintained at 363 K for five days. After this time, the mixture was cooled and the resulting precipitate was filtered and washed repeatedly with water and acetone to remove the free surfactant. The light-yellow powder was dried at 333 K for 1 day and then calcined at temperatures of 723–1173 K (ramp rate 10 K/min) for at least 2 h under air flow. No residual halogens were present on the samples after drying and calcination.

2.2. Characterization

Powder X-ray data were collected with a Siemens powder diffractometer using Cu-Kα radiation (λ=1.5418Å) by placing samples in aluminum sample holders. High-resolution powder XRD data for structural analysis were collected over a 14 h period from 2Θ=20–75 with a 0.02° step size.

Conventional transmission electron microscopy combined with dispersive X-ray microanalysis (EDX) was carried out with a Hitachi H 800-MT electron microscope working at 200 kV and equipped with a Kevex analytical system. Samples were supported on carbon-coated gold grids by depositing a drop of the specimen suspended in methanol. The sample was then transported to the microscope stage and the equipment was pumped down for several hours before observation.

The Raman spectra were taken on a Bio-rad Digilab Division dedicated FT-Raman spectrometer between 3500 and 70 cm^{-1} at 4 cm^{-1} optical resolution employing 500 mW energy of a Nd:YVO_4 excitation laser at the sample position. Glass capillary sample holders were used. A total of 512 accumulated scans were taken. The spectra were processed employing the GRAMS/386-based software supplied with the FT-Raman spectrometer.

Textural properties and porosity were measured with a Carlo Erba Sorptomatic 1900 instrument interfaced to a computer. Surface area and pore size distribution were calculated using, respectively, B.E.T. and Dollimore/Heal methods.

3. Results and discussion

The approach we used for the preparation of mesoporous, high surface area ceria–zirconia exploits the interaction of the mixture of hydrous oxides with cationic surfactants under basic conditions. The method derives from the observation that hydrous oxide can exchange either cations or anions, depending on the pH of the medium. It has been recently reported that hydrous zirconium oxide effectively incorporates cationic surfactants at a pH well above its isoelectric point, allowing a partial degree of ordering to develop over time [20]. Pure ZrO_2 samples with a surface area in the range 240–360 m^2/g were prepared with this method by varying the chain length of the surfactant. The isoelectric point of hydrous zirconium oxide in aqueous solution (6.7) is close to that of cerium (6.75) [24] and slightly dependent on the environment. In accordance with these features the following equilibrium can be delineated for Ce, Zr and a mixture of the two (Scheme 1).

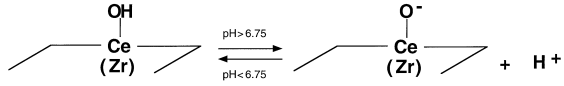

Scheme 1.

Conducting the precipitation of hydrous mixed oxide at a pH>8 in the presence of cationic surfactant should permit the cation exchange process between H^+ and the surfactant together with the formation of an inorganic/organic composite which upon calcination will originate a mesoporous mixed-oxide phase. The strong similarity of the isoelectric points of Zr and Ce would enable exchangeable sites to be equally distributed over the surface and the extent of substitution of the hydroxy groups to be comparable.

The hydrous oxides prepared according to the method described in the Section 2 are easily isolated from the system by filtration and water washing. These materials generally contain a large amount of alkylammonium even after thorough washing. The presence of surfactant is clearly observed by combined FTIR/TG-DTA experiments and elemental analysis. Fig. 1(a) shows an FTIR spectrum of $Ce_{0.68}Zr_{0.32}O_2$ after washing and drying at 333 K for 15 h. The sample shows typical adsorption bands in the regions of 2900–2800 cm^{-1} and 1600 cm^{-1}, corresponding to the stretching and bending modes of the surfactant

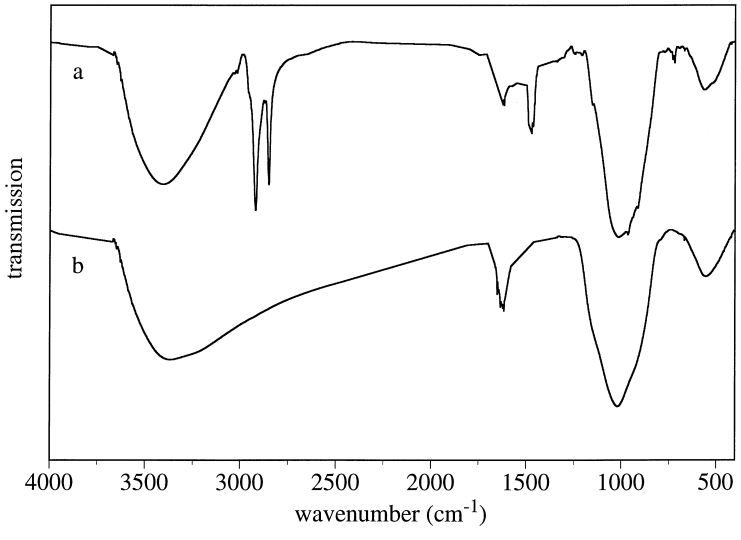

Fig. 1. FTIR spectra of (a) CZ68 dried at 333 for 24 h and (b) CZ68 calcined at 723 K under air flow for 2 h.

hydrocarbon chain. Carbon/nitrogen atomic ratios, measured by elemental analysis, are consistent with the presence of surfactant, which remains intact during synthesis. The amount of water and surfactant retained after drying are consistent with a material of composition $Ce_{0.68}Zr_{0.32}O_x(O–C_{16}H_{42}N)_{\sim 0.1}\cdot 0.8H_2O$. Elimination of water and the organics takes place in the range of temperatures between 400 and 600 K. After calcination for 2 h at 723 K, no residual C or N is detected on the surface and the IR spectrum is consistent with the complete removal of the surfactant (Fig. 1(b)). Other bands in the IR spectrum of Fig. 1(a) are due to the presence of residual OH from water (3500 cm^{-1}, 1600 cm^{-1}) and to the stretching of Zr(Ce)–O bands (550 cm^{-1}). The strong band at 1000 cm^{-1} is probably associated with adsorbed carbonates.

The powder X-ray diffractogram of the materials were collected before and after calcination. Neither CZ80 nor CZ68 exhibit reflections at low 2Θ angles, indicating the absence of a long-range order with regular pore distribution. This is not in agreement with the report of Hudson and Knowles [20], who observed a partial ordering in pure ZrO_2 which disappeared upon calcination. This difference is likely to be related to the presence, in our case, of a Ce-rich phase, which may change the thermal stability of the mesostructured mixed-oxide composites, probably as a result of the different oxo-chemistries of cerium and zirconium. For example, a lower degree of Ce–Zr–O condensation could lead to less developed inorganic/organic composites. In addition, the existence of more than one stable oxidation state in cerium could lead to structural collapse following the redox process in solution and during calcination. The cerium cation in high-surface area cerium oxide is known to be easily reducible even at room temperature under particular conditions [12]. The addition of Zr increases the low temperature reduction features of ceria; therefore it is likely that the development of a regular mesoscopic organization is hindered by the redox of cerium (Ce^{3+}–Ce^{4+}). For example, reduction of Ce^{4+} operated by the incorporated surfactant could lead to structural collapse during calcination.

X-ray diffraction patterns after calcination indicate the presence of a true mixed-oxide phase with the cubic, fluorite structure typical of CeO_2 (Fig. 2). There is no indication of the presence of other phases. Calculation of the cell parameters was carried out using the six main reflections typical of a fluorite-structured material with a fcc cell, corresponding to the {111}, {200}, {220}, {311}, {222} and {400} planes. Values of a=0.5375(6)nm and a=0.5346(9)nm were obtained for CZ80 and CZ68, respectively. These

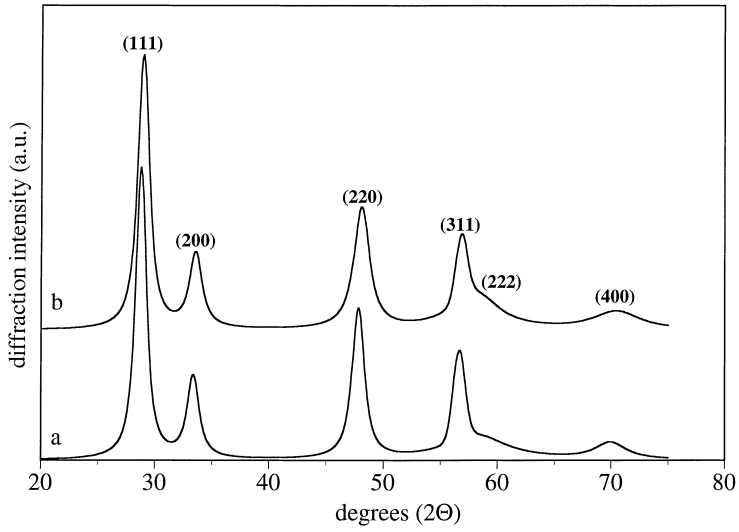

Fig. 2. X-ray diffraction pattern of (a) CZ80 and (b) CZ68 calcined at 1173 K for 2 h.

results are in agreement with those obtained from Ce–Zr–O prepared by other routes and are consistent with calculations made from empirical relationships [25]. The ceria–zirconia system is rather complex. Several phases were detected, depending on composition. $Ce_xZr_{1-x}O_2$ crystallizes into a cubic structure if x is higher than 0.5, whereas a tetragonal cell is preferred for $0.2<x<0.5$ and a monoclinic phase is observed at the higher ZrO_2 content. A tetragonal cell (with $c/a=1$) deriving from a cubic cell with a slight displacement of oxygen anion from their ideal fluorite sites has been also observed at composition in the range $0.2<x<0.5$ [26]. This phase is generally referred as a cubic phase because its XRD pattern is indexed in the cubic Fm3m space group [4]. The presence of a cubic-only phase in our sample is in agreement with the above observations and also indicates that Ce and Zr are homogeneously distributed (the presence of Ce- or Zr-rich domains would lead to preferential formation of more than one phase). The lack of free ZrO_2 is also confirmed by Raman spectroscopy. The Raman spectrum of $Ce_{0.68}Zr_{0.32}O_2$ is shown in Fig. 3, where it is compared with that of pure CeO_2 prepared by conventional precipitation. There is only one strong adsorption peak centered at 462 cm^{-1} typical of the F_{2g} Raman active mode of a fluorite-structured material, with a broad scattering between 100 and 700 cm^{-1}. The different intensity of the band in the two samples may originate from the different degree of porosity and crystallinity of CeO_2 (surface area 74 m^2/g) and ceria–zirconia (surface area 115 m^2/g). No bands characteristic of pure ZrO_2 were detected.

3.1. TEM–EDX studies

The homogeneity and morphology of our samples was also investigated by TEM–EDX studies. All samples have a similar morphology and exhibit a very narrow particle-size histogram. The mean particle size for each sample is reported in Table 1. Samples treated at 1173 K show a larger particle size than those treated at lower temperatures, as expected. Fig. 4 corresponds to the $Ce_{0.68}Zr_{0.32}O_2$ sample treated at 923 K, for example, where the degree of morphological homogeneity is complete. The chemical homogeneity of all samples was checked by obtaining the Zr/Ce ratio of individual particles (which are too small to perform any individual compositional profile), using an electron probe of about 5 nm in diameter. In each case, more than 150 individual particles were analyzed. The results for each sample have been summarized by

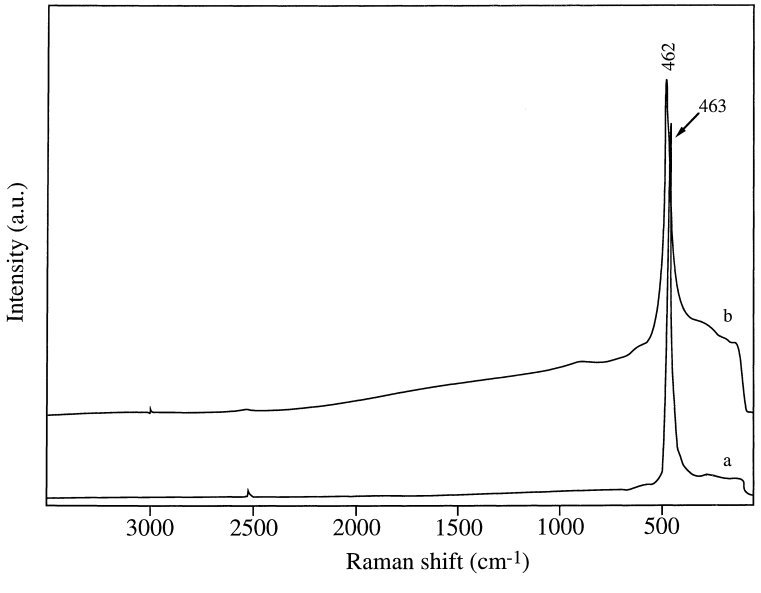

Fig. 3. Raman spectra of (a) pure CeO_2 and (b) CZ68 calcined at 1073 K.

Table 1
Mean particle size distribution and chemical composition obtained from combined TEM–EDX measurements (probe size of 5 nm)

Sample	Calcination temperature (K)	Mean particle size (nm)	Average Zr/Ce atomic ratio
$Ce_{0.80}Zr_{0.20}O_2$	923	8–10	0.254
$Ce_{0.80}Zr_{0.20}O_2$	1173	15–18	0.263
$Ce_{0.68}Zr_{0.32}O_2$	923	4–6	0.472
$Ce_{0.68}Zr_{0.32}O_2$	1173	13–15	0.475

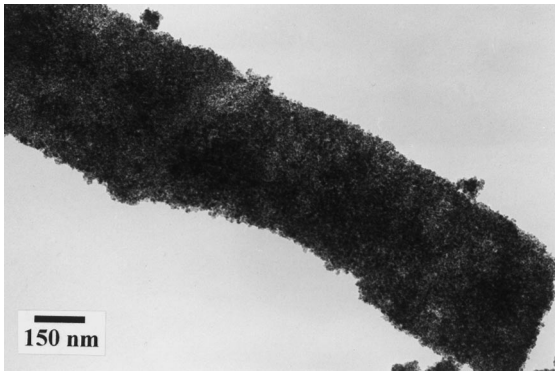

Fig. 4. Transmission electron micrograph of CZ68 treated at 923 K showing a complete morphological homogeneity.

plotting the Zr/Ce atomic ratio obtained from EDX analysis vs the number of individual particles which show the given Zr/Ce value (Fig. 5 and 6). From these diagrams, an average Zr/Ce atomic ratio, also included in Table 1, can be calculated for each sample. The average Zr/Ce atomic ratios found experimentally by EDX are in close agreement with the theoretical values, 0.25 and 0.471 for $Ce_{0.8}Zr_{0.2}O_2$ and $Ce_{0.68}Zr_{0.32}O_2$, respectively. It is important to note that no isolated CeO_2 and ZrO_2 particles were found in this case, indicating a high degree of solid solution formation. However, the chemical homogeneity of particles making up the sample is not complete, as can be deduced from Fig. 5 and Fig. 6. The degree of chemical homogeneity is related to the treatment temperature. As the calcination temperature increases, the samples becomes more chemically homogeneous, thus indicating that sintering of particles is also accompanied by compositional homogenization.

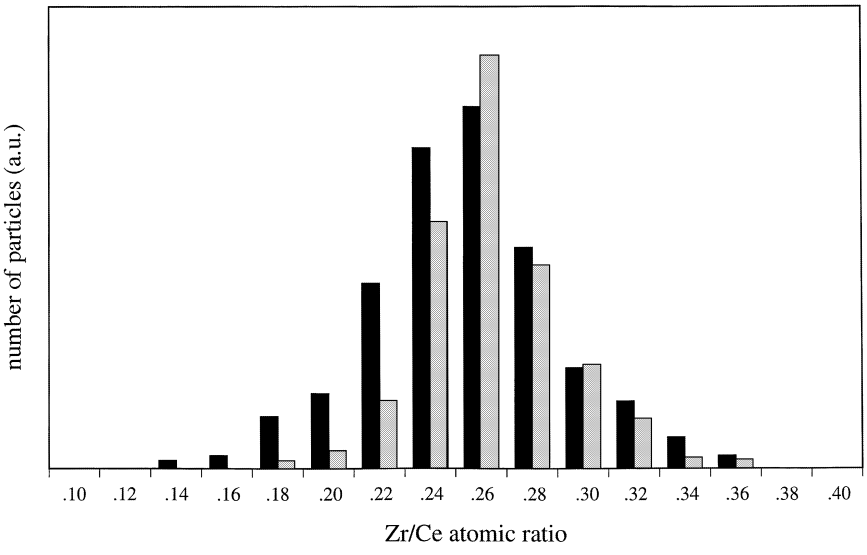

Fig. 5. Zr/Ce atomic ratio obtained from EDX analysis vs number of individual particles for CZ80 treated at 923 K (black bar) and at 1173 K (gray bar).

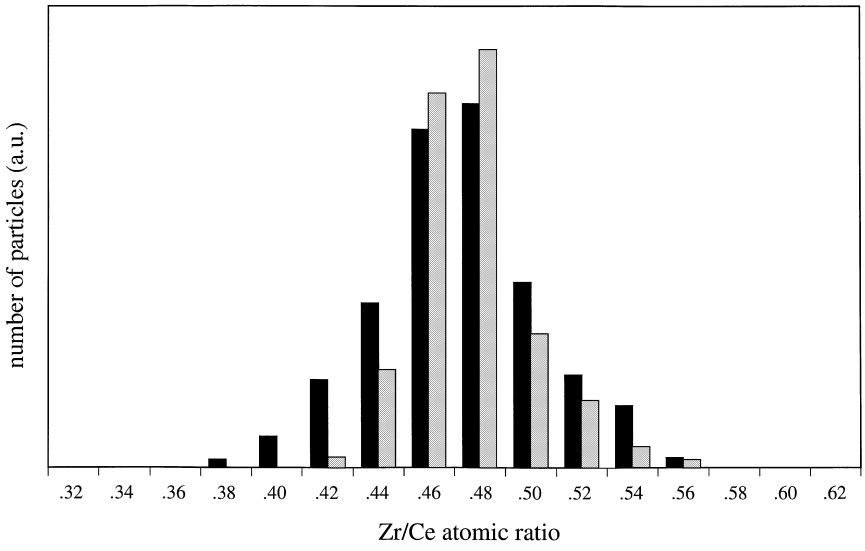

Fig. 6. Zr/Ce atomic ratio obtained from EDX analysis vs number of individual particles for CZ68 treated at 923 K (black bar) and at 1173 K (gray bar).

3.2. Textural and adsorption studies

Nitrogen adsorption/desorption studies were carried out on samples treated at different temperatures in order to investigate the effect of calcination on surface area and porosity. Textural properties are summarized in Table 2. The minimum calcination temperature was 723 K. At this temperature, all the organics were desorbed from the surface and no residual C or N was detected. Surface areas in excess of 200 m^2/g were observed for both CZ80 and CZ68 and, as expected, surface area decreased at higher temperatures. However, surface area values are still appreciable after calcination at 1173 K. Surface area of CZ80 prepared using surfactants compares favorably with that of samples prepared by conventional co-precipitation (see Table 2), and to the best of our knowledge, these are the highest surface areas reported for ceria–zirconia after calcination in the range 773–1100 K. These values are lower than those found with pure ZrO_2 under similar conditions, but they become closer if we bear in mind the mass difference between Ce and Zr. Using the same methodology, pure ceria with a surface area of 190 m^2/g

Table 2
BET surface areas and total pore volume of solid solutions as a function of calcination temperature

Sample	Calcination temperature [a] (K)	Surface area (m^2/g)	Pore volume (cm^3/g)
$Ce_{0.80}Zr_{0.20}O_2$	723	208 (103)[b]	0.86 (0.194)[b]
	923	163 (85)	0.56 (0.09)
	1073	124 (56)	0.49 (0.15)
	1173	56 (23)	0.13 (0.03)
$Ce_{0.68}Zr_{0.32}O_2$	723	235	0.66
	923	170	0.42
	1073	115 (113)[c]	0.21
	1173	40	0.07

[a] The material was hold for 2 h under air flow at the temperature indicated.
[b] In parenthesis is reported the value obtained with $Ce_{0.80}Zr_{0.20}O_2$ prepared by conventional co-precipitation.
[c] Value obtained after 40 h of treatment.

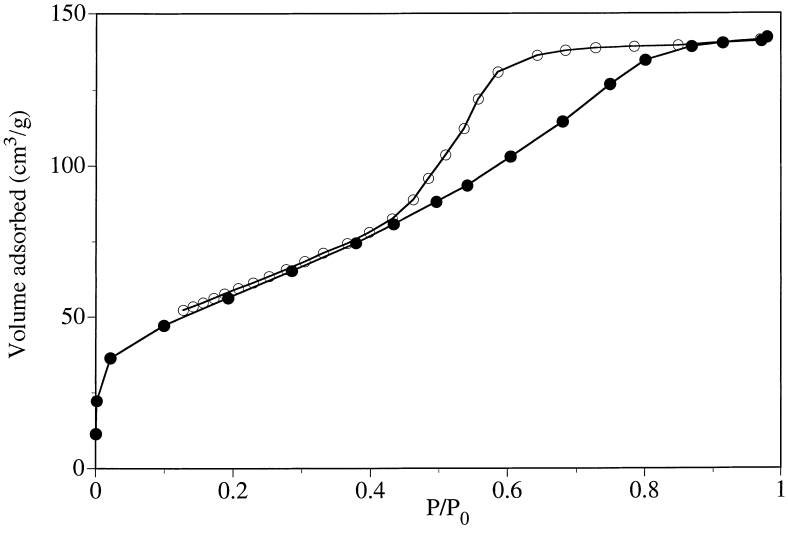

Fig. 7. Nitrogen adsorption isotherm at 77.4 K for a sample of CZ68 treated at 723 K.

after calcination at 773 K has been obtained [27]. The introduction of ZrO_2, therefore, slightly stabilizes the surface area of ceria, in agreement with the results obtained on catalysts prepared by conventional routes [10]. This is probably due to the inhibition of the sintering process induced by a dopant ion.

Nitrogen adsorption/desorption experiments revealed all the materials to be porous. The N_2 isotherms of all powders were of type IV, typical of a mesoporous sample (Fig. 7). Pore-size distribution curves calculated from the desorption branch of the isotherms indicate the presence of mesoporosity although they do not evidence the presence of regularly ordered pores, in agreement with the lack of diffraction peaks at low 2Θ angles. This indicates the formation of materials of a different class, where mesoporosity is not lost, but there is a pore formation mechanism that differs from that observed in MCM and similar materials. A maximum for pore distribution was observed at around 2 nm (Fig. 8) and this value is not shown to be appreciably affected by changes in the chain length of the surfactant (from C_{14} to C_{18}). The absence of microporosity can be deduced from the *t*-plot shown in Fig. 9. A surface of 228 (close to the B.E.T. value of 235 m^2/g) is calculated using the relation $t(\text{Å}) = \{13.99/[\log(\frac{P_0}{P}) + 0.034]\}^{1/2}$. The absence of a positive intercept indicates that all of the surface is associated with mesoporosity. The low value of the B.E.T. constant *c* in all samples ($80<c<100$) is another indication of the absence of microporosity.

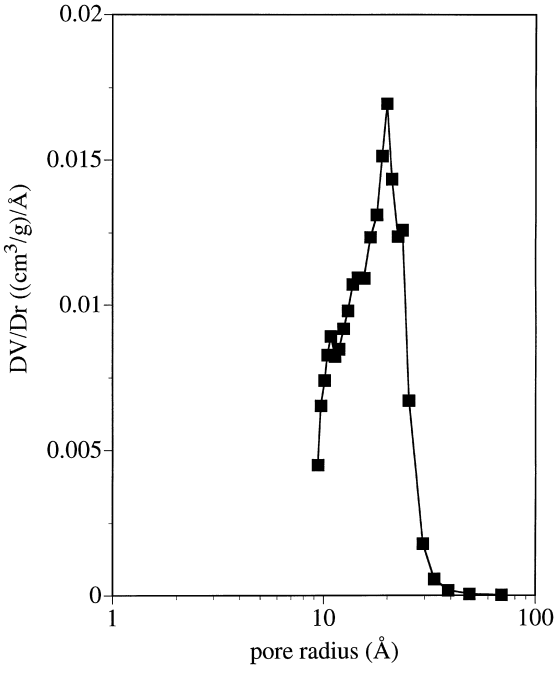

Fig. 8. Pore-size distribution for a sample of CZ68 treated at 723 K.

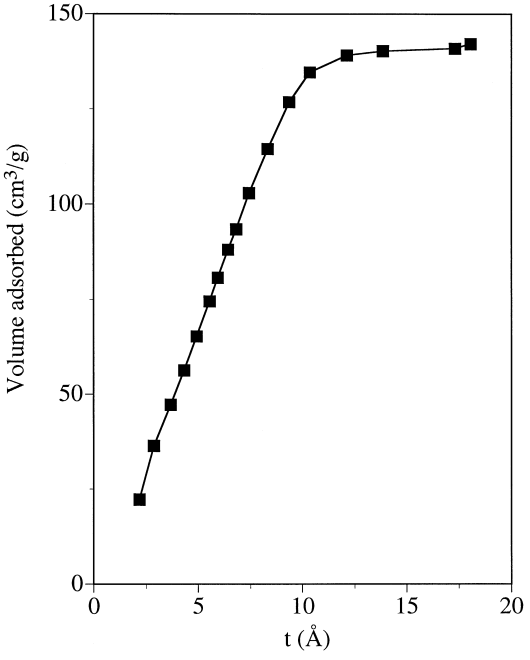

Fig. 9. '*t*-plot' obtained from the adsorption branch of the isotherm of Fig. 7 calculated using the relation $\{13.99/[\log(\frac{P_0}{P}) + 0.034]\}^{1/2}$.

The influence of various synthesis parameters like (i) the pH of the medium and (ii) the nature of surfactant on the surface area was also investigated. The effective incorporation of the organics into the hydrous oxide is requested for the surfactant to modify textural properties of the resulting oxide. Reaction conducted at a pH of 11.5 for 5 days gives the highest surface area. At lower pH values, the degree of incorporation of the surfactant is lower, owing to the presence of fewer surface OH groups available for exchange. This will result in a less developed pore-structure with a drop in surface area. Thus, a sample of CZ68 obtained from reaction carried out at a pH of 9 had a surface area of 136 m^2/g, and the degree of incorporation of surfactant was reduced. The dried material had a composition of $Ce_{0.68}Zr_{0.32}O_x(O–C_{16}H_{42}N)_{\sim 0.06}\cdot 0.9H_2O$ indicating that only 0.06 mol of surfactant per mol of metal (total Ce+Zr) were incorporated. This means that for a surface area of 200 m^2/g, assuming a cubic structure, approximately 0.3 mol of surfactant are incorporated per mol of exposed metal (surface Ce+Zr) [28]; a value which is lower than that reported in [20] for pure ZrO_2. The degree of incorporation of the surfactant and the homogeneity of solid solutions are also dependent on reaction times, being lower for reaction times of less than 2–3 days. This is probably due to an incomplete exchange reaction between the hydroxy groups of the hydrous oxide and the surfactant.

Overall, the results presented in this paper do not show any evidence for the formation of a regular 3D-structure although the incorporation of the surfactant enhances the values of surface areas available for ceria–zirconia. In addition, the mixed oxides show a good compositional homogeneity and thermal stability, which is an important requirement in these materials for applications in the formulation of catalysts for auto-exhaust treatment.

Therefore alternative explanations, which do not rely on the formation of regular pores, should be given to support and explain these findings. It is likely that the incorporation of surfactants reduces the surface tension of water even in the absence of a partial degree of ordering. As a matter of fact, surfactants can be added to the pore liquid to reduce the interfacial energy and thereby decrease the surface tension of water contained in the pores. This will reduce the shrinkage and collapse of the network during drying and calcination, which could help to maintain high surface areas.

Acknowledgements

Financial support from CNR and MURST (Rome) is acknowledged. We are also indebt to Dr. J. Kiss for carrying out Raman spectra.

References

[1] A. Trovarelli, C. de Leitenburg, G. Dolcetti, CHEMTECH 6 (1997) 32.
[2] P. Fornasiero, R. Di Monte, G. Ranga Rao, J. Kašpar, S. Meriani, A. Trovarelli, M. Graziani, J. Catal. 151 (1995) 168.
[3] T. Murota, T. Hasegawa, S. Aozasa, H. Matsui, M. Motoyama, J. Alloys Comp. 193 (1993) 298.
[4] P. Fornasiero, G. Balducci, R. Di Monte, J. Kašpar, V. Sergo, G. Gubitosa, A. Ferrero, M. Graziani, J. Catal. 164 (1996) 173.
[5] F. Zamar, A. Trovarelli, C. de Leitenburg, G. Dolcetti, Stud. Surf. Sci. Catal. 101 (1996) 1283.

[6] M. Pijolat, M. Prin, M. Soustelle, O. Touret, P. Nortier, J. Chem. Soc. Faraday Trans. 91 (1995) 3941.
[7] F. Zamar, A. Trovarelli, C. de Leitenburg, G. Dolcetti, J. Chem. Soc. Chem. Comm. (1995) 965.
[8] G. Ranga Rao, P. Fornasiero, R. Di Monte, J. Kašpar, G. Vlaic, G. Balducci, S. Meriani, G. Gubitosa, A. Cremona, M. Graziani, J. Catal. 162 (1996) 1.
[9] A. Trovarelli, F. Zamar, J. Llorca, C. de Leitenburg, G. Dolcetti, J. Kiss, J. Catal. 169 (1997) 490.
[10] C. de Leitenburg, A. Trovarelli, G. Bini, F. Cavani, J. Llorca, Appl. Catal. A: General 139 (1996) 161.
[11] C.E. Hori, H. Permana, K.Y.S. Ng, A. Brenner, K. More, K.M. Rahmoeller, D. Belton, Appl. Catal. B: Environ. Appl. Catal. B: 16 (1998) 105.
[12] A. Trovarelli, Catal. Rev.- Sci. Eng. 38 (1996) 439.
[13] Y. Sun, P.A. Sermon, J. Mater. Chem. 6 (1996) 1025.
[14] C.T. Kresge, M.E. Leonowicz, W.J. Roth, J.C. Vartuli, J.S. Beck, Nature 359 (1992) 710.
[15] Q. Huo, D.I. Margolese, U. Ciesla, P. Feng, T.E. Gier, P. Sieger, R. Leon, P.M. Petroff, B. Schüth, G.D. Stucky, Nature 368 (1994) 317.
[16] P.T. Tanev, T.J. Pinnavaia, Science 267 (1995) 865.
[17] U. Ciesla, S. Schacht, G.D. Stucky, K.K. Unger, F. Schüth, Angew. Chem. Int. Ed. Engl. 35 (1996) 541.
[18] D.M. Antonelli, J.Y. Ying, Angew. Chem. Int. Ed. Engl. 35 (1996) 426.
[19] Q. Huo, D.I. Margolese, U. Ciesla, D.G. Demuth, P. Feng, T.E. Gier, P. Sieger, A. Firouzi, B.F. Chmelka, B. Schüth, G.D. Stucky, Chem. Mater. 6 (1994) 1176.
[20] M.J. Hudson, J.A. Knowles, J. Mater. Chem. 6 (1996) 89.
[21] J.S. Reddy, A. Sayari, Catal. Lett. 38 (1996) 219.
[22] G. Larsen, E. Lotero, M. Nabity, L.M. Petkovic, D.S. Shobe, J. Catal. 164 (1996) 246.
[23] A. Kim, P. Bruinsma, Y. Chen, L.-Q. Wang, J. Lin, Chem. Commun. (1997) 161.
[24] G.A. Parks, Chem. Rev. 65 (1965) 177.
[25] D.J. Kim, J. Am. Ceram. Soc. 72 (1989) 1415.
[26] M. Yashima, H. Arashi, M. Kakihana, M. Yoshimura, J. Am. Ceram. Soc. 77 (1994) 1067.
[27] D. Terribile, A. Trovarelli, C. de Leitenburg, G. Dolcetti J. Llorca, Chem. Mater. Chem. Mater. 9 (1997) 2676.
[28] M.F.L. Johnson, J. Mooi, J. Catal. 103 (1987) 502.